1 **Title**: MexEF-OprN multidrug efflux pump transporter negatively controls *N*-acyl-homoserine lactone

2 accumulation in *Pseudomonas syringae* pv. *tabaci* 6605

3

4 **Authors' names**: Takahiro Sawada[1], Miho Eguchi[1], Seiya Asaki[2], Ryota Kashiwagi[2], Kousuke Shimomura[2],

5 Fumiko Taguchi[1,3], Hidenori Matsui[1], Mikihiro Yamamoto[1], Yoshiteru Noutoshi[1], Kazuhiro Toyoda[1] and Yuki

6 Ichinose[1,*]

7

8 **Running title**: MexEF-OprN negatively regulates AHL production

9

10 **Affiliation and address**:

11 [1]Graduate School of Environmental and Life Science, Okayama University, Tsushima-naka 1-1-1, Kita-ku,

12 Okayama 700-8530, Japan

13 [2]Faculty of Agriculture, Okayama University, Tsushima-naka 1-1-1, Kita-ku, Okayama 700-8530, Japan

14 [3]Present address: Department of Biotechnology, Graduate School of Engineering, Nagoya University, Furo-cho,

15 Chikusa-ku, Nagoya 464-8603, Japan

16 ***For correspondence**: E-mail yuki@okayama-u.ac.jp; Tel/Fax: (+81) 86 251 8308.

17

18

19 **Number of figures and Tables**: 6 figures, 3 tables (3 supplemental figures)

20 **Words counts**: 5864 (text) + 571 (Tables)

21 **Nucleotide sequence accession numbers**: AB676069 for *mexT* and LC217528 for *mexEFoprN*, respectively

22

23   **Abstract** (219 words)

24   Our previous studies revealed that flagellar motility-defective mutants such as Δ*fliC* of *Pseudomonas syringae*

25   pv. *tabaci* 6605 (*Pta*6605) have remarkably reduced production of *N*-acyl-homoserine lactones (AHL), quorum

26   sensing molecules. To investigate the reason of loss of AHL production in Δ*fliC* mutant, we carried out

27   transposon mutagenesis. Among approximately 14,000 transconjugants, we found 11 AHL

28   production-recovered (APR) strains. In these APR strains, a transposon was inserted into either *mexE* or *mexF*,

29   genes encoding for the multidrug efflux pump transporter MexEF-OprN, and *mexT*, a gene encoding a putative

30   transcriptional activator for *mexEF-oprN*. These results suggest that MexEF-OprN is a negative regulator of

31   AHL production. To confirm the negative effect of MexEF-OprN on AHL production, loss- and

32   gain-of-function experiments for *mexEF-oprN* were carried out. The Δ*fliC*Δ*mexF* and Δ*fliC*Δ*mexT* double

33   mutant strains recovered AHL production, whereas the *mexT* overexpressing strain abolished AHL production,

34   although the *psyI*, a gene encoding AHL synthase is transcribed as wild-type. Introduction of a *mexF* or *mexT*

35   mutation into another flagellar motility- and AHL production–defective mutant strain, Δ*motCD*, also recovered

36   the ability to produce AHL. Furthermore, introduction of the *mexF* mutation into other AHL production–

37   defective mutant strains such as Δ*gacA* and Δ*aefR* also recovered AHL production but not to the Δ*psyI* mutant.

38   These results indicate that MexEF-OprN is a decisive negative determinant of AHL production and

39   accumulation.

40

41

42   **Keywords**: *N*-Acyl-homoserine lactone, Flagella motility, MexEF-OprN, Multidrug efflux pump transporter,

43   Quorum sensing

44

Introduction

Pseudomonas syringae is an economically important phytopathogenic bacterium that has been isolated from a wide variety of plant species. It can be classified into at least 50 pathovars on the basis of its host plant species and type of disease symptoms (Sawada et al. 1999). *P. syringae* is also one of the most well studied phytopathogenic bacteria, and complete genome sequences of three model strains, *P. syringae* pv. *tomato* DC3000 (Buell et al. 2003), *P. syringae* pv. *syringae* B728a (*Pss*B728a, Feil et al. 2005) and *P. syringae* pv. *phaseolicola* 1448A (Joardar et al. 2005), were determined at the beginning in the 21st century. Thus, almost all effector genes were identified, and significant numbers of functions of effectors have been investigated (http://www.pseudomonas-syringae.org). Nowadays, in addition to the above three strains, complete genome sequences of at least 22 strains of *P. syringae* have been assembled, and draft genome sequences of more than 454 strains of *P. syringae* have been published including that of *P. syringae* pv. *tabaci* 6605 (*Pta*6605), a causal agent of tobacco wild fire disease (http://www.ncbi.nlm.nih.gov/assembly/organism/136849/all/). Nevertheless, it is still largely unknown how virulence-related gene expression is regulated.

We have long investigated virulence factors in *Pta*6605, and found that the flagellin-defective mutant Δ*fliC* lost abilities to swim and to produce quorum-sensing molecules, *N*-acyl-homoserine lactones (AHL) (Ichinose et al. 2013; Shimizu et al. 2003; Taguchi et al. 2010). We also generated other types of flagellar motility defective mutants; Δ*motCD*, a mutant of flagellar stator protein MotCD (Kanda et al. 2011), and Δ*fgt1*, a mutant for the flagellar glycosyltransferase FGT1 (Taguchi et al. 2010), and found that both mutants also largely reduced or lost the ability to produce AHL (Kanda et al. 2011; Taguchi et al. 2010). Furthermore, the Δ*gacA*, a mutant for GacA response regulator of the GacSA two component system, and the Δ*aefR*, a mutant of one of TetR transcription factor family remarkably reduced AHL production (Kawakita et al. 2012; Marutatni et al. 2008). These results suggest that flagellar motility, GacSA two component system and AefR transcription factor are required for AHL production, and there might be a complex regulatory system for AHL production.

In this study, we investigated why the Δ*fliC* mutant of *Pta*6605 lost the ability to produce AHL. As a result of screening the clones that had recovered AHL production by transposon mutagenesis, we determined that the multidrug efflux pump transporter MexEF-OprN, a member of the resistance-nodulation-division (RND) family of Gram-negative bacteria (Li and Nikaido, 2009), negatively regulates AHL production. The mechanism and relationship between AHL production and the function of MexEF-OprN will be discussed.

Materials and methods

75 **Bacterial strains and growth condition**

76 All bacterial strains used in this study are listed in Table 1. The *Pta*6605 strains were maintained as described

77 (Taguchi et al. 2006). The *Escherichia coli* strains were grown at 37°C in Luria-Bertani (LB) medium

78 (Sambrook et al. 1989). *Chromobacterium violaceum* CV026 was grown at 30°C in LB with kanamycin at a

79 final concentration of 50 µg/ml (McClean et al. 1997).

80 **Transposon mutagenesis**

81 Previous studies reported that the Δ*fliC* mutant of *Pta*6605 had lost almost all AHL production (Taguchi et al.

82 2010). In this study, we introduced a transposon into the Δ*fliC* mutant, then screened colonies that had

83 recovered the ability to produce AHL. The transposon plasmid vector, pBSLC1 (Fig. 1), was constructed by

84 ligation of a wide-range transposon vector, pBSL118 (Alexeyev et al. 1995), and the conventional vector

85 pHSG396 (Takara, Shiga Japan) at the *Eco*RI site. The transposon was introduced into the Δ*fliC* mutant by

86 conjugation with *E. coli* S17-1 that possessed pBSLC1, and the region from "I" to "O" was integrated into the

87 Δ*fliC* chromosome. Replica plates for all transconjugants were made, and overnight-cultured *C. violaceum*

88 CV026 was overlaid after mixing with 0.6% agar LB medium. After an additional overnight incubation at 30°C,

89 AHL production was visualized as violacein pigment.

90 **Plasmid rescue of transposon-integrated regions from AHL production recovered (APR) strains and**

91 **sequencing analysis to identify insertion sites**

92 Genomic DNA of AHL production–recovered (APR) strains was purified according to the method of Wilson

93 (1989) and digested with *Hin*dIII. The resultant DNA was ligated using a Ligation-Convenience Kit (Nippon

94 Gene, Tokyo Japan), then introduced into ECOS™-competent *E. coli* DH5α (Nippon Gene, Tokyo, Japan).

95 Plasmid DNA was purified from the transformants, and transposon-inserted sites were identified by sequencing

96 with the M13 Fw primer.

97 **Extraction and detection of AHLs**

98 Extraction of AHLs and their detection using *C. violaceum* CV026 were performed as described previously

99 (Taguchi et al. 2010). Briefly, *Pseudomonas* strains were cultured overnight in King's B (KB) medium (King et

100 al. 1954) or LB medium supplemented with 10 mM $MgCl_2$ and mixed with the same amount of ethyl acetate,

101 then the ethyl acetate extract containing AHL was evaporated. The pellet was dissolved in a small amount of

102 ethyl acetate, then spotted on a C_{18} reversed-phase thin layer chromatography (TLC) plate (TLC Silica gel 60,

103 Merck, Darmstadt, Germany). After the spotted ethyl acetate had dried, the overnight culture of biosensor

104   bacterium *C. violaceum* CV026 was mixed with 0.6% agar LB medium and overlaid. The plates were incubated

105   at 30°C, and the violet pigment violacein was observed as production of AHLs.

106   **Extraction of total RNA and analysis of gene expression**

107   Total RNA was extracted using a Total RNA Purification Kit (Jena Bioscience, Jena, Germany) from the cells

108   collected by centrifugation. The cDNA was synthesized using ReverTra Ace® qPCR RT Master Mix with

109   gDNA Remover (Toyobo, Osaka, Japan) according to the manufacturer's instructions. Semi-quantitative

110   Reverse Transcriptase (RT)-PCR analysis was conducted using 0.5 µg of total RNA. The specific primer sets for

111   continuous transcript from kanamycin resistant gene to *psyI* (Km-F and *psyI*-R1) in APR10, for *mexT* (*mexT*-F1

112   and *mexT*-R1), *mexE* (*mexE*-F1 and *mexE*-R1) and *psyI* (*psyI*-F and *psyI*-R) were designed according to the

113   registered sequences of *Pta*6605 (Table 2). PCR was performed as follows: one denaturation cycle of 2 min at

114   94°C, indicated cycles in each figure legend of 10 s at 98°C, 30 s at 55°C, and 15 s at 68°C using 1/10 of RT

115   product and KOD FX Neo (Toyobo). A half volume of the PCR product (10 µl) was loaded on 2% agarose gel.

116   RT-PCR was also carried out without reverse transcription as a negative control.

117   **Generation of *lux* box deletion mutant**

118   The genetic region containing *lux* box and surrounding region was amplified by PCR using a set of PCR primers,

119   *lux*-1 and *lux*-2 (Table 2) with KOD FX DNA polymerase (Toyobo, Tokyo), then dAMP (deoxyadenosine

120   monophosphate) was added to the 3' end of the PCR product with 10 × A-attachment mix (Toyobo), then

121   inserted into a pGEM-T Easy vector (Promega, Tokyo, Japan). Using a recombinant plasmid DNA, pGEM-*lux*,

122   as a template, inverse PCR was carried out using a set of PCR primers, d*lux*-3 and d*lux*-4 to delete a *lux* box

123   from *psyI* promoter. Then the PCR product and template DNA were digested with *Bam*HI and *Dpn*I. The

124   resultant DNA was self-ligated with T4 DNA ligase (Ligation-convenience kit, Nippon Gene, Tokyo). The *lux*

125   box-deleted DNA construct was introduced into the *Eco*RI site of the mobilizable cloning vector pK18*mobsacB*

126   (Schäfer et al. 1994), and used for conjugation and homologous recombination.

127   **Introduction of *mexF* and *mexT* mutations into *Pta*6605 wild-type and various mutant strains**

128   To introduce the *mexF* mutation, the genetic region for *mexF* was amplified using a set of PCR primers, *mexF*-F

129   and *mexF*-R (Table 2), that were designed based on the sequence of *Pta*6605 provided by Dr. D. Studholme,

130   University of Exeter, UK (Fig. 2A), then inserted into a pGEM-T Easy vector (Promega, Tokyo, Japan). The

131   recombinant plasmid obtained was digested with *Msc*I and *Bsp*1407I to delete the internal 1240 bp for

132   generation of the Δ*mexF* mutant plasmid, treated with S1-nuclease to generate blunt ends, and self-ligated by a

133   Ligation-Convenience kit (Nippon Gene). The mutated genetic region was introduced into a pK18*mobsacB*

134 plasmid via an *Eco*RI site to generate pK18-Δ*mexF*, then transformed into *E. coli* S17-1 for conjugation with

135 *Pta*6605 strains. For introduction of the *mexT* mutation into various mutant strains such as Δ*fliC*, Δ*motCD*, and

136 Δ*psyI* of *Pta*6605, *E. coli* S17-1 possessing pK18-Δ*mexT* (Kawakita et al. 2012) was used for conjugation.

137 Deletion mutants were obtained by conjugation and homologous recombination according to the previously

138 reported methods (Taguchi et al. 2006). The DNA sequence of the mutated region in the bacterium was

139 confirmed by DNA sequencing with a BIG Dye terminator cycle sequencing kit and an ABI PRISM 3100

140 sequencer (Applied Biosystems, Chiba, Japan).

141 **Heterologous expression of *mexT***

142 To evaluate the effect of heterologous expression of *mexT* on AHL production in *Pta*6605, we first isolated the

143 *mexT* gene using a set of PCR primers, *Bam*HI-*mexT* and *mexT*-*Eco*RI (Table 2), and genomic DNA of *Pta*6605,

144 then the *Bam*HI/*Eco*RI-digested *mexT* fragment was introduced into a broad host range plasmid vector,

145 pDSK519 (Keen et al. 1988). *Pta*6605 wild-type, *Pta*6605 (pDSK519), or *Pta*6605 (pDSK519-*mexT*) were

146 cultured overnight in LB supplemented with 10 mM $MgCl_2$. Bacterial density was adjusted to an OD_{600} of 1.6

147 with KB, then 200 μl of bacterial suspension was inoculated into 3 ml of LB medium supplemented with 10

148 mM $MgCl_2$ with or without isopropyl β-D-1-thiogalactopyranoside (IPTG) at a final concentration of 1.0 mM.

149 Bacteria were incubated for 5 h at 27°C for RNA purification and another overnight for AHL extraction.

150

151 **Results**

152 **Screening of APR strains by transposon mutagenesis and identification of genes in which transposons**

153 **were inserted**

154 To screen potential negative regulatory genes for AHL production in the *Pta*6605 Δ*fliC* mutant, we conjugated

155 *Pta*6605 Δ*fliC* and *E. coli* S17-1 possessing a transposon vector, pBSLC1 (Fig. 1). The AHL production of

156 approximately 14,000 independent transconjugants was assessed using *C. violacerum* CV026. Among them, 11

157 strains were isolated as APR strains. As shown in Fig. S1, although the Δ*fliC* mutant lost AHL production, all

158 APR strains recovered AHL production equal to the wild-type strain. To identify the genes into which the

159 transposon was inserted we rescued plasmid DNA containing the pHSG396-derived ColE1 replication origin,

160 chloramphenicol-resistant gene and integrated region of genomic DNA in each APR strain. Sequencing analysis

161 using an M13-Fw primer revealed that among 11 APR strains, 1, 7, and 2 APR strains had transposon insertions

162 in *mexE*, *mexF*, and their putative transcriptional activator gene, *mexT*, respectively (Fig. 2AC). MexT is a

163 LysR-type transcription factor and is known to positively regulate transcription of *mexEF-oprN* in *Pseudomonas*

164 *aeruginosa* (Fetar et al. 2011; Köhler et al. 1999; Maseda et al. 2004).

165   Furthermore, we found one more transposon insertion in APR10 just in a *lux* box in a promoter region of

166 *psyI* (Fig. 2B). Because *lux*-box is destroyed by the transposon insertion, activated transcription of the *psyI*

167 promoter is independent of the *lux* box in APR10. The *lux* box was initially identified in a *luxI* promoter of

168 *Vibrio fischeri* (Devine et al. 1988), and it conserves an imperfect 20 bp inverted repeat with relatively low

169 stringency. The *luxI* transcription was positively regulated by the cognate transcription factor, LuxR (Sitnikov et

170 al. 1995). We found that the kanamycin resistance gene upstream of *psyI* locates at the same orientation with

171 *psyI* in APR10. Therefore, *psyI* might be transcribed from the promoter of the kanamycin resistance gene. To

172 further confirm the continuous transcript from kanamycin resistance gene to *psyI*, we carried out RT-PCR

173 analysis using total RNA prepared from APR10. RT-PCR analysis was carried out using a set of primers, Km-F

174 and *psyI*-R1 with/without reverse transcription. Genomic DNA of wild-type strain and APR10 was used as a

175 template DNA for negative and positive control, respectively. About 280 bp of PCR product was appeared when

176 genomic DNA of APR10 was used as a template, but not that of wild-type strain (Fig. 3A). A PCR product of

177 the same size also appeared with RT-PCR of APR10, but did not appear without RTase treatment. We cloned

178 PCR product and sequencing analysis confirmed the expected sequence (Fig. 3B).

179   To reveal involvement of *lux* box of *psyI* transcription in *Pta*6605, we generated Δ*lux* box mutant in

180 *Pta*6605, and investigated AHL accumulation (Fig S2). Although wild-type *Pta*6605 produced significant level

181 of AHL, the Δ*lux* box mutant did not produce any detectable AHL.

182 **AHL production in double mutant strains of flagellar genes such as *fliC, motCD*, and**

183 **MexEF-OprN-related genes such as *mexF* and *mexT***

184 Because transposon mutagenesis suggested that MexEF-OprN and its positive regulator MexT are negative

185 regulators of AHL production, we generated double mutant strains, Δ*fliC*Δ*mexF* and Δ*fliC*Δ*mexT*, as

186 representative mutants of both flagellar motility and the MexEF-OprN multidrug efflux pump system, and

187 investigated AHL production. As shown in Fig. 4A, both double mutants recovered AHL production, and we

188 confirmed that MexEF-OprN negatively regulated AHL production. The single mutation of *mexF* did not affect

189 AHL production, as we observed in the Δ*mexT* mutant (Kawakita et al. 2012).

190   As we showed a part of the microarray analysis of AHL production-defective mutants (Table 3, Taguchi

191 et al. 2015), not only the Δ*fliC* mutant but also another flagellar motility-defective mutant, Δ*motCD*, reduced the

192 expression of *psyI* and *psyR*, and also enhanced that of *mexEF-oprN* genes (Kanda et al. 2011). We carried out

193 semi-quantitative RT-PCR of *mexE* (Fig. S3), and confirmed activation of *mexE* expression in Δ*fliC*, Δ*motCD*,

194 Δ*psyI* and Δ*aefR* mutant strains. These results indicate some relationship between AHL production and

195 MexEF-OprN activity. To clarify it we generated the double mutant strains Δ*motCD*Δ*mexF* and Δ*motCD*Δ*mexT*

196 and found both these mutant strains recovered AHL production ability (Fig. 4A). Therefore, we confirmed that

197 MexEF-OprN and MexT were negative regulators of AHL production. In this experiment, we also examined the

198 AHL production in Δ*psyI*Δ*mexF* and Δ*psyI*Δ*mexT* double mutant strains. As we expected, neither mutant

199 recovered AHL production, indicating that PsyI is an indispensable protein for AHL production (Fig. 4A).

200 **AHL production in double mutant strains Δ*gacA*Δ*mexF*, Δ*aefR*Δ*mexF*, and corresponding single mutant**

201 **strains.**

202 It is known that the GacSA two-component system and transcriptional factor AefR are required for AHL

203 production in *P. syringae* (Cha et al. 2012; Kawakita et al. 2012; Marutani et al. 2008; Quiñones et al. 2004;

204 Yun et al. 2015). As shown in Table 3, microarray analysis suggested that *psyI* expression was remarkably

205 reduced in both Δ*aefR* and Δ*gacA* mutant strains. Most AHL production-defective mutants such as Δ*psyI*, Δ*fliC*,

206 Δ*motABCD*, and Δ*aefR* up-regulated *mexEF-oprN* gene expression, and Δ*aefR* especially extremely activated

207 *mexEF-oprN* gene expression (Taguchi et al. 2015). However, unlike these mutant strains, *mexEF-oprN* gene

208 expression in the Δ*gacA* mutant was not significantly affected (Table 3 and Fig. S3). To clarify the involvement

209 of MexEF-OprN in AHL production in Δ*aefR* and Δ*gacA* mutant strains, we examined AHL production in

210 Δ*aefR*Δ*mexF* and Δ*gacA*Δ*mexF* double mutants. As shown in Fig. 4B, almost no AHL was detected in the

211 Δ*aefR* mutant, whereas the level of AHL production was significantly reduced in the Δ*gacA* mutant in

212 comparison with the wild-type strain, as we previously reported (Kawakita et al. 2012; Marutani et al. 2008).

213 However, with introduction of the *mexF* mutation, both Δ*aefR*Δ*mexF* and Δ*gacA*Δ*mexF* recovered AHL

214 production to nearly the wild-type level (Fig. 4B).

215 **Effect of *mexT* overexpression on AHL production**

216 To investigate the effect of overexpression of *mexEF-oprN* on AHL production, the broad-host-range plasmid

217 vector pDSK519 with or without *mexT* was introduced into the *Pta*6605 wild-type strain. Although *mexT* was

218 inserted at the multicloning site of pDSK519 under control of a *lac* promoter, we observed almost the same

219 level of *mexT* and *mexE* transcripts in *Pta*6605 possessing pDSK519-*mexT* with and without treatment of 1.0

220 mM IPTG by RT-PCR analysis. Because this system lacked the *lacI*, a gene for LacI repressor protein, the

221 addition of IPTG had no effect on *mexT* expression and AHL production. We did not detect these transcripts in

222 *Pta*6605 possessing a pDSK519 empty vector or not possessing *Pta*6605 (Fig. 5A). Using these bacterial strains,

223   AHL was detected by *C. violaceum* CV026 in both wild-type and strain possessing a pDSK519 empty vector,

224   but not in the pDSK519-*mexT*-possessing strain (Fig. 5B). These results clearly showed that expression of *mexT*

225   resulted in the activation of *mexEF-oprN* and consequently abolished AHL production. We also examined *psyI*

226   expression by RT-PCR analysis (Fig. 5A). Unexpectedly, *psyI* expression was unaffected by *mexT* expression.

227

228   **Discussion**

229   **Role of *lux* box and PsyR on AHL production in *Pta*6605**

230   The orthologues of *luxI* and *luxR* were identified as *psmI* and *psmR* in *P. syringae* pv. *maculicola* strain CFBP

231   10912–9 (Elasri et al. 2001), as *ahlI* and *ahlR* in *Pss*B728a (Quiñones et al. 2004), and as *psyI* and *psyR* in

232   *Pta*6605, and *lux* box consensus sequences were found at positions -76 to -57 upstream of the *psmI* and *psyI*

233   start codons and -77 to -58 upstream of the *ahlI* start codon, respectively (Fig. 2B). LuxR with AHL is known to

234   bind to a *lux* box in *V. fischeri* as a transcriptional activator (Sitnikov et al. 1995). However another LuxR type

235   transcription factor, EasR in *Pantoea stewartii* is known to bind homologous *lux* box (*esa* box) without AHL as

236   a transcriptional repressor (Minogue et al. 2002). In *P. syringae* although the binding of PsyR to a *lux* box is not

237   investigated yet, this study clearly revealed that *lux* box is required for *psyI* transcription, and therefore PsyR is

238   a transcriptional activator of *psyI* via *lux* box binding.

239   **MexT, a transcriptional activator for *mexEF-oprN***

240   In our previous study, we examined the effect of *mexT* mutation in *Pta*6605, and reported that the Δ*mexT* mutant

241   retained the ability to produce AHL and did not show remarkable changes in in vitro growth or virulence

242   (Kawakita et al. 2012). Therefore, we expected that MexT is not involved in the regulation of *mexEF-oprN*

243   expression and AHL production. However, the result obtained in this study revealed that each mutation of *mexE*,

244   *mexF* and *mexT* in Δ*fliC* mutant recovered AHL production (Fig. 4). Now we assume that these contradictory

245   results were due to the level of *mexEF-oprN* gene expression in wild-type stain (Kawakita et al. 2012) and Δ*fliC*

246   mutant in this study. Kawakita et al. (2012) compared the phenotypes of Δ*mexT* mutant and wild-type strains in

247   which *mexEF-oprN* expression was almost silenced, whereas this study analyzed the effect of *mexF* mutation of

248   the Δ*fliC* mutant in which *mexEF*-oprN expression was extremely activated (Taguchi et al. 2010).

249   In this study, we observed that overexpression of *mexT* induced the expression of *mexE* (Fig. 5A), and

250   mutation of *mexT* recovered AHL production in the mutant strains (Fig. 4A). From these results it is clear that

251   MexT is an activator of *mexEF-oprN*. However, RT-PCR analysis of *mexT* in the wild-type strain and AHL

252   production-defective mutant strains revealed that *mexT* is similarly expressed in all strains examined (Fig. S3).

253 This result indicates that expression of *mexEF-oprN* may not be simply regulated by MexT only at least in the

254 wild-type and Δ*gacA* mutant strains. Thus, the regulation of *mexEF-oprN* expression seems to be complex, and

255 needs further study.

256 **Role of MexEF-OprN on AHL production**

257 In this study, we found the defect of MexEF-OprN, one of the multidrug efflux pump transporters, resulted in

258 the recovery of AHL production in Δ*fliC*, Δ*motCD*, Δ*gacA* and Δ*aefR* mutants (Fig. 4). In other words, the

259 MexEF-OprN multidrug efflux pump transporter functions as a negative regulator of AHL production in these

260 mutants. We also found that activation of *mexEF-oprN* resulted in the loss of AHL production (Fig. 5). This

261 result led us to speculate that MexEF-OpeN actively excretes AHL even at lower concentrations, and this

262 interferes with its accumulation. The expression of *psyI* was at an equal level in the *mexT*-overexpressed strain,

263 wild-type and strains possessing pDSK519 empty vector (Fig. 5). This result indicates that the activation of

264 MexEF-OprN influenced on the accumulation of AHL, not the transcription of *psyI*. Thus, level of *psyI*

265 transcription is independent of MexEF-OprN activity. The expression of *mexEF-oprN* in Δ*fliC*, Δ*motCD* and

266 Δ*aefR* is upregulated, but not in Δ*gacA* (Table 3, Fig. S3). Because Δ*gacA*Δ*mexF* mutant also recovered AHL

267 production (Fig. 4), MexEF-OprN negatively regulates AHL accumulation also in Δ*gacA*. GacA seems to

268 regulate AHL accumulation dependent on and independent of MexEF-OprN (Fig. 6). GacS/GacA

269 two-component system is known to activate transcription of *rsmX* and *rsmY,* genes for small noncoding RNA in

270 bacterial density-dependent manner in *P. fluorescens* (Humair et al. 2010). GacS/GacA two-component system

271 positively controls the quorum-sensing response in *P. aeruginosa*, and both *gacA* mutant and *rsmY rsmZ* double

272 mutant were similarly impaired in the synthesis of AHL (Kay et al. 2006). Because *P. syringae* pv. *tomato*

273 DC3000 and other pathovars also conserve *rsmX*, *rsmY* and *rsmZ* genes (Moll et al. 2010), it may be possible

274 that AHL accumulation is also regulated via Gac/Rsm signal transduction pathway.

275 As mentioned above, overexpression of MexEF-OprN abrogates AHL accumulation. However,

276 microarray analysis of the Δ*psyI* mutant also revealed that *mexEF-oprN* was upregulated in the Δ*psyI* mutant

277 (Taguchi et al. 2015; Table 3 and Fig. S3), indicating that AHL suppressed the activation of *mexEF-oprN* gene

278 expression (Fig. 6). Although we observed that overexpressed *mexEF-oprN* interfered with AHL accumulation

279 in *Pta*6605, it was reported that the MexEF-OprN efflux pump exports a *Pseudomonas* quinolone signal (PQS)

280 precursor, 4-hydroxy-2-heptylquinoline, which is one of the quorum sensing signals in *P. aeruginosa*. Therefore,

281 PQS is poorly synthesized in the mutants constitutively expressing *mexEF-oprN* in *P. aeruginosa* (Lamarche

282 and Déziul 2011). Furthermore, transcription of *rhlI*, a gene encoding C4-homoserine lactone autoinducer

283 synthase is largely decreased in the *mexEF-oprN* overexpressing *P. aeruginosa* strain (Köhler et al. 2001). Thus,

284 the export of autoinducers by MexEF-OprN might be common among *Pseudomonas* species. However, unlike

285 the mutant strains, the natural function of MexEF-OprN in the infection process of the wild-type strain is not

286   known yet. It is also unclear whether MexEF-OprN excretes another substance besides AHL. The study of the

287   effects of MexEF-OprN on virulence is now underway.

288   **Relationship between flagellar motility and expression of *mexEF-oprN***

289   Because the Δ*gacA* mutant lost and Δ*aefR* mutant remarkably reduced swarming motility (Kawakita et al. 2012;

290   Marutani et al. 2008), and all flagellar-motility-defective mutant strains lost or reduced AHL production (Kanda

291   et al. 2011; Taguchi et al. 2010), flagellar motility might be necessary for AHL production (Fig. 6).

292   Flagellar-motility-defective mutant strains might be mimic of bacteria in a late stage of infection. Bacteria in the

293   biofilm on plant cell surface may be able to sense flagella immobility and respond by shutting down AHL

294   production. Although we identified that elevated activity of the MexEF-OprN multidrug efflux pump transporter

295   caused the loss of AHL production, it is still unclear why *mexEF-oprN* expression was increased in flagellar

296   motility-defective mutant strains such as Δ*fliC*. Because non-motile bacteria need to adapt to given environment,

297   activation of an efflux pump transporter seems to be reasonable and plausible strategy to survive. It's a

298   remaining subject to elucidate how bacteria recognize that they cannot move and need to escape from an

299   unsuitable environment.

300

306

307   **Compliance with ethical standards**

308   **Conflict of interest**

309   All of the authors declare that they have no conflict of interest.

310   **Ethical approval**

311   This article does not contain any studies with animals performed by any of the authors.

312

313   **References**

314   Alexeyev MF, Shokolenko IN, Croughan TP (1995) New mini-Tn5 derivatives for insertion mutagenesis and

315   genetic engineering in gram-negative bacteria. Can J Microbiol 41:1053-1055

316   Buell CR, Joardar V, Lindeberg M, Selengut J, Paulsen IT, Gwinn ML, Dodson RJ, Deboy RT, Durkin AS,

317   Kolonay JF, Madupu R, Daugherty S, Brinkac L, Beanan MJ, Haft DH, Nelson WC, Davidsen T, Zafar

318 N, Zhou L, Liu J, Yuan Q, Khouri H, Fedorova N, Tran B, Russell D, Berry K, Utterback T, Van Aken

319 SE, Feldblyum TV, D'Ascenzo M, Deng WL, Ramos AR, Alfano JR, Cartinhour S, Chatterjee AK,

320 Delaney TP, Lazarowitz SG, Martin GB, Schneider DJ, Tang X, Bender CL, White O, Fraser CM,

321 Collmer A (2003) The complete genome sequence of the *Arabidopsis* and tomato pathogen

322 *Pseudomonas syringae* pv. *tomato* DC3000. Proc Natl Acad Sci USA 100:10181-10186

323 Cha JY, Lee DG, Lee JS, Oh JI, Baik HS (2012) GacA directly regulates expression of several virulence genes

324 in *Pseudomonas syringae* pv. *tabaci* 11528. Biochem Biophys Res Commun 417:665–672

325 Devine JH, Countryman C, Baldwin TO (1988) Nucleotide sequence of the *luxR* and *luxI* genes and structure of

326 the primary regulatory region of the *lux* regulon of *Vibrio fischeri* ATCC 7744. Biochemistry 27:837-842

327 Elasri M, Delorme S, Lemanceau P, Stewart G, Laue B, Glickmann E, Oger PM, Dessaux Y (2001)

328 Acyl-homoserine lactone production is more common among plant-associated *Pseudomonas* spp. than

329 among soilborne *Pseudomonas* spp. Appl Environ Microbiol 67:1198-1209

330 Feil H, Feil WS, Chain P, Larimer F, DiBartolo G, Copeland A, Lykidis A, Trong S, Nolan M, Goltsman E,

331 Thiel J, Malfatti S, Loper JE, Lapidus A, Detter JC, Land M, Richardson PM, Kyrpides NC, Ivanova N,

332 Lindow SE (2005) Comparison of the complete genome sequences of *Pseudomonas syringae* pv.

333 *syringae* B728a and pv. *tomato* DC3000. Proc Natl Acad Sci USA 102:11064-11069

334 Fetar H, Gilmour C, Klinoski R, Daigle DM, Dean CR, Poole K (2011) *mexEF-oprN* multidrug efflux operon of

335 *Pseudomonas aeruginosa*: regulation by the MexT activator in response to nitrosative stress and

336 chloramphenicol. Antimicrob Agents Chemother 55:508-514

337 Humair B, Wackwitz B, Haas D (2010) GacA-controlled activation of promoters for small RNA genes in

338 *Pseudomonas fluorescens*. Appl Environ Microbiol 76:1497-1506

339 Ichinose Y, Taguchi F, Mukaihara T (2013) Pathogenicity and virulence factors of *Pseudomonas syringae*. J

340 Gen Plant Pathol 79:285-296

341 Joardar V, Lindeberg M, Jackson RW, Selengut J, Dodson R, Brinkac LM, Daugherty SC, Deboy R, Durkin AS,

342 Giglio MG, Madupu R, Nelson WC, Rosovitz MJ, Sullivan S, Crabtree J, Creasy T, Davidsen T, Haft

343 DH, Zafar N, Zhou L, Halpin R, Holley T, Khouri H, Feldblyum T, White O, Fraser CM, Chatterjee AK,

344 Cartinhour S, Schneider DJ, Mansfield J, Collmer A, Buell CR (2005) Whole-genome sequence analysis

345 of *Pseudomonas syringae* pv. phaseolicola 1448A reveals divergence among pathovars in genes involved

346 in virulence and transposition. J Bacteriol 187:6488-6498

347   Kanda E, Tatsuta T, Suzuki T, Taguchi F, Naito K, Inagaki Y, Toyoda K, Shiraishi T, Ichinose Y (2011) Two

348   flagellar stators and their roles in motility and virulence in *Pseudomonas syringae* pv. *tabaci* 6605. Mol

349   Genet Genomics 285:163-174

350   Kawakita Y, Taguchi F, Inagaki Y, Toyoda K, Shiraishi T, Ichinose Y (2012) Characterization of each *aefR* and

351   *mexT* mutant in *Pseudomonas syringae* pv. *tabaci* 6605. Mol Genet Genomics 287:473-484

352   Kay E, Humair B, Dénervaud V, Riedel K, Spahr S, Eberl L, Valverde C, Haas D (2006) Two GacA-dependent

353   small RNAs modulate the quorum-sensing response in *Pseudomonas aeruginosa*. J Bacteriol

354   188:6026-6033

355   Keen NT, Tamaki S, Kobayashi D, Trollinger D (1988) Improved broad-host-range plasmids for DNA cloning

356   in Gram-negative bacteria. Gene 70:191-197

357   King EO, Ward NK, Raney DE (1954) Two simple media for the demonstration of pyrocyanin and fluorescein.

358   J Lab Clin Med 44:301-307

359   Köhler T, Epp SF, Curty LK, Pechère J-C (1999) Characterization of MexT, the regulator of the

360   MexE-MexF-OprN multidrug efflux system of *Pseudomonas aeruginosa*. J Bacteriol 181:6300–6305

361   Köhler T, van Delden C, Curty LK, Hamzehpour MM, Pechere JC (2001) Overexpression of the MexEF-OprN

362   multidrug efflux system affects cell-to-cell signaling in *Pseudomonas aeruginosa*. J Bacteriol

363   183:5213-5222

364   Lamarche MG, Déziel E (2011) MexEF-OprN efflux pump exports the *Pseudomonas* quinolone signal (PQS)

365   precursor HHQ (4-hydroxy-2-heptylquinoline). PLoS One 6:e24310

366   Li XZ, Nikaido H (2009) Efflux-mediated drug resistance in bacteria: an update. Drugs 69:1555-1623

367   Marutani M, Taguchi F, Ogawa Y, Hossain MM, Inagaki Y, Toyoda K, Shiraishi T, Ichinose Y (2008) Gac

368   two-component system in *Pseudomonas syringae* pv. *tabaci* is required for virulence but not for

369   hypersensitive reaction. Mol Genet Genomics 279:313-322

370   Maseda H, Sawada I, Saito K, Uchiyama H, Nakae T, Nomura N (2004) Enhancement of the *mexAB-oprM*

371   efflux pump expression by a quorum-sensing autoinducer and its cancellation by a regulator, MexT, of

372   the *mexEF-oprN* efflux pump operon in *Pseudomonas aeruginosa*. Antimicrob Agents Chemother

373   48:1320-1328

374   McClean KH, Winson MK, Fish L, Taylor A, Chhabra SR, Camara M, Daykin M, Lamb JH, Swift S, Bycroft

375   BW, Stewart GS, Williams P (1997) Quorum sensing and *Chromobacterium violaceum*: exploitation of

376   violacein production and inhibition for the detection of *N*-acylhomoserine lactones. Microbiology

377   143:3703-3711

378 Minogue TD, Wehland-von Trebra M, Bernhard F, von Bodman SB (2002) The autoregulatory role of EsaR, a

379   quorum-sensing regulator in *Pantoea stewartii* ssp. *stewartii*: evidence for a repressor function. Mol

380   Microbiol 44:1625-1635

381 Moll S, Schneider DJ, Stodghill P, Myers CR, Cartinhour SW, Filiatrault MJ (2010) Construction of an *rsmX*

382   co-variance model and identification of five *rsmX* non-coding RNAs in *Pseudomonas syringae* pv.

383   *tomato* DC3000. RNA Biol 7:508-516

384 Quiñones B, Pujol CJ, Lindow SE (2004) Regulation of AHL production and its contribution to epiphytic fitness

385   in *Pseudomonas syringae*. Mol Plant-Microbe Interact 17:521-531

386 Sambrook T, Fritshch EF, Maniatis J (1989) Molecular Cloning: A Laboratory Manual. Cold Spring Harbor

387   Laboratory Press, Cold Spring Harbor, NY

388 Sawada H, Suzuki F, Matsuda I, Saitou N (1999) Phylogenetic analysis of *Pseudomonas syringae* pathovars

389   suggests the horizontal gene transfer of *argK* and the evolutionary stability of *hrp* gene cluster. J Mol

390   Evol 49:627-644

391 Schäfer A, Tauch A, Jäger W, Kalinowski J, Thierbach G, Pühler A (1994) Small mobilizable multi-purpose

392   cloning vectors derived from the *Escherichia coli* plasmids pK18 and pK19: selection of defined

393   deletions in the chromosome of *Corynebacterium glutamicum*. Gene 145:69-73

394 Shimizu R, Taguchi F, Marutani M, Mukaihara T, Inagaki Y, Toyoda K, Shiraishi T, Ichinose Y (2003) The

395   Δ*fliD* mutant of *Pseudomonas syringae* pv. *tabaci,* which secretes flagellin monomers, induces a strong

396   hypersensitive reaction (HR) in non-host tomato cells. Mol Genet Genomics 269:21-30

397 Sitnikov DM, Schineller JB, Baldwin TO (1995) Transcriptional regulation of bioluminesence genes   from

398   *Vibrio fischeri*. Mol Microbiol 17:801-812

399 Taguchi F, Inoue Y, Suzuki T, Inagaki Y, Yamamoto M, Toyoda K, Noutoshi Y, Shiraishi T, Ichinose Y (2015)

400   Characterization of quorum sensing-controlled transcriptional regulator MarR and Rieske (2Fe-2S)

401   cluster-containing protein (Orf5), which are involved in resistance to environmental stresses in

402   *Pseudomonas syringae* pv. *tabaci* 6605. Mol Plant Pathol 16:376-387

403 Taguchi F, Takeuchi K, Katoh E, Murata K, Suzuki T, Marutani M, Kawasaki T, Eguchi M, Katoh S, Kaku H,

404   Yasuda C, Inagaki Y, Toyoda K, Shiraishi T, Ichinose Y (2006) Identification of glycosylation genes and

405   glycosylated amino acids of flagellin in *Pseudomonas syringae* pv. *tabaci*. Cell Microbiol 8:923-938

406 Taguchi F, Yamamoto M, Ohnishi-Kameyama M, Iwaki M, Yoshida M, Ishii T, Konishi T, Ichinose Y (2010)

407   Defects in flagellin glycosylation affect the virulence of *Pseudomonas syringae* pv. *tabaci* 6605.

408   Microbiology 156:72-80

409 Wilson K (1989) Preparation of genomic DNA from bacteria, in: Ausubel FM, Brent R, Kingston RE, Moor DD,

410   Smith JA, Seidman JG, Struhl K (Eds.), Current Protocols in Molecular Biology, John Wiley and Sons,

411   New York, NY, pp. 2.4.1-2.4.5

412 Yun S, Lee JS, Do MS, Jeon YJ, Cha JY, Baik HS (2015) Functional analysis of the *aefR* mutation and

413   identification of its binding site in *Pseudomonas syringae* pv. *tabaci* 11528. Acta Biochim Biophys Sin

414   47:938–945

415

416   **Figure legends**

417   **Fig. 1** Structure of plasmid pBSLC1 used for transposon mutagenesis. Plasmid is not drawn to scale. One of the

418   general-purpose plasmid vectors, pHSG396, and transposon vector pBSL118 were ligated at *Eco*RI. The region

419   between "I" and "O" is randomly inserted into the bacterial genome. The *oriV* and ColE1 *ori* are replication

420   origins of R6K and colicin E1 plasmids, respectively, and *oriT* is an RP4 plasmid-derived conjugative transfer

421   origin. The *tnp* encodes transposase. Amp, ampicillin; Cm, chloramphenicol; Km, kanamycin. The position and

422   direction of the M13-Fw primer are indicated by arrow.

423   **Fig. 2** Schematic organization of genes into which transposons were inserted. (A) Insertion sites of a transposon

424   in *mexEFoprN* operon and *mexT* gene. There are 1, 7, and 2 insertions in *mexE*, *mexF*, and *mexT*, respectively.

425   Insertion sites are indicated by arrows. Generation of *mexF* mutant is also indicated. (B) Insertion site of a

426   transposon in the *psyI* promoter. The *lux* box, translation start codon ATG, is indicated together with the

427   transposon insertion site. The *lux* boxes from *P. syringae* pv. *maculicola* strain CFBP 10912–9 (*Psm*, Elasri *et*

428   *al*., 2001), *P. syringae* pv. *syringae* B728a (PssB728a, Quiñones *et al*., 2004), and *Vibrio fischeri* ATCC7744

429   (Devine *et al*., 1988) are also shown. Arrows below the sequences indicate imperfect inverted repeats. The

430   nucleotides identical to the *lux* box in *Pta*6605 are white on a black background. (C) Insertion sites of all APR

431   strains.

432   **Fig. 3** RT-PCR analysis of transcript between kanamycin resistance gene and *psyI* in APR10. (A) Genomic

433   DNA (G) of *Pta*6605 wild-type and APR10 was used for PCR as a template. The RT-PCR was carried out using

434   APR10 RNA with/without reverse transcription. Fastgene 50 bp DNA Ladder (Nippon Genetics, Co. LTD,

435   Tokyo Japan) was used as a size marker. (B) Sequence of PCR product. Positions of PCR primers are shown in

436   italic, and part of *lux* box sequence is boxed. The doubly and singly underlined sequences are part of open

437   reading frames for kanamycin resistance gene and *psyI*, respectively. Amino acid sequences are shown below

438   nucleotide sequences. The nucleotide sequence is numbered from side of kanamycin resistance gene.

439   **Fig. 4** AHL production in the double mutant strains. AHL was visualized as described in Materials and Methods.

440   (A) Ethyl acetate extract from 1 ml of bacterial culture from Δ*fliC*Δ*mexF*, Δ*motCD*Δ*mexF*, Δ*psyI*Δ*mexF*.

441   Δ*fliC*Δ*mexT*, Δ*motCD*Δ*mexT*, and Δ*psyI*Δ*mexT*, and corresponding single mutant strains and wild-type strain

442   was spotted on the TLC plate. (B) Ethyl acetate extract from 1.5 ml of bacterial culture from Δ*fliC*Δ*mexF*,

443   Δ*gacA*Δ*mexF*, Δ*aefR*Δ*mexF* and corresponding single mutant strains and wild-type strain was spotted on the

444   TLC plate.

445   **Fig. 5** Effect of *mexT*-overexpression on AHL production. (A) Semi-quantitative RT-PCR of *mexT*, *mexE* and

446   *psyI*. PCR for *mexT* and *mexE* was cycled for 25 times, and that for *psyI* was cycled for 30 times. Fastgene 50

447   bp DNA Ladder (Nippon Genetics) was used as a size marker. (B) AHL production. Ethyl acetate extract from 2

448   ml of each bacterial culture was spotted on the TLC plate. AHL was visualized as described in Materials and

449   Methods.

450   **Fig. 6** Schematic depiction of regulatory network for AHL production in *Pta6605*.

451

Table 1. Bacterial strains and plasmids used in this study

Bacterial strain or plasmid	Relevant characteristics	Reference or source
E. coli strain		
DH5α	*F⁻ λ⁻ ø80dLacZΔM15 Δ(lacZYA-argF)U169 recA1 endA1 hsdR17 (rK⁻mK⁺) supE44 thi-1gyrA relA1*	Takara, Kyoto, Japan
S17-1	*thi pro hsdR⁻hsdM⁺recA* [*chr*::RP4-2-*Tc*::Mu-*Km*::Tn7]	Schäfer *et al.* (1994)
P. syringae pv. *tabaci*		
Isolate 6605	Wild-type, Nal^r	Shimizu et al. (2003)
6605-Δ*fliC*	Isolate 6605 Δ*fliC*, Nal^r	Shimizu et al. (2003)
6605-APR series	Isolate 6605 Δ*fliC*::mini-Tn5, Nal^r, Km^r, Cm^r	This study
6605-Δ*mexF*	Isolate 6605 Δ*mexF*, Nal^r	This study
6605-Δ*mexT*	Isolate 6605 Δ*mexT*, Nal^r	Kawakita et al. (2012)
6605-Δ*motCD*	Isolate 6605 Δ*motCD*, Nal^r	Kanda et al. (2011)
6605-Δ*gacA*	Isolate 6605 Δ*gacA*, Nal^r	Marutani et al. (2008)
6605-Δ*aefR*	Isolate 6605 Δ*aefR*, Nal^r	Kawakita et al. (2012)
6605-Δ*psyI*	Isolate 6605 Δ*psyI*, Nal^r	Taguchi et al. (2010b)
6605-Δ*lux* box	Isolate 6605 Δ*lux* box, Nal^r	This study
6605-Δ*fliCΔmexF*	Isolate 6605 Δ*fliCΔmexF*, Nal^r	This study
6605-Δ*motCDΔmexF*	Isolate 6605 Δ*gacAΔmexF*, Nal^r	This study
6605-Δ*psyIΔmexF*	Isolate 6605 Δ*aefRΔmexF*, Nal^r	This study
6605-Δ*fliCΔmexT*	Isolate 6605 Δ*fliCΔmexF*, Nal^r	This study
6605-Δ*motCDΔmexT*	Isolate 6605 Δ*gacAΔmexF*, Nal^r	This study
6605-Δ*psyIΔmexT*	Isolate 6605 Δ*aefRΔmexF*, Nal^r	This study
6605-Δgac*AΔmexF*	Isolate 6605 Δ*fliCΔmexF*, Nal^r	This study
6605-Δ*aefRΔmexF*	Isolate 6605 Δ*gacAΔmexF*, Nal^r	This study
Plasmid		
pGEM-T Easy	Cloning vector, Amp^r	Promega, Madison, WI, USA
pGEM-*lux*	pGEM-T Easy possessing 1929-bp *lux* box and surrounding regions, Amp^r	This study
pGEM-*mexF*	pGEM-T Easy possessing 3210-bp *mexF* and surrounding regions, Amp^r	This study
pGEM-*mexT*	pGEM-T Easy possessing 2177-bp *mexT*, Amp^r	This study
pK18*mobsacB*	Small mobilizable vector, Km^r, sucrose-sensitive (*sacB*)	Schäfer *et al.* (1994)
pK18-Δ*mexF*	*Eco*RI-digested *mexF* fragment with 1240 bp deletion containing pK18*mobsacB*, Km^r	This study
pK18-Δ*mexT*	*Eco*RI-digested *mexT* fragment with 163 bp deletion containing pK18*mobsacB*, Km^r	Kawakita *et al.* (2012)
pDSK519	Broad-host-range cloning vector, Km^r	Keen et al. (1988)

pDSK519-*mexT*	pDSK519 possessing expressible *mexT*, Km^r	This study
pBSL118	Mini-Tn5-derived plasmid vector for insertion mutagenesis, Amp^r, Km^r	Alexeyev *et al.* (1995)
pBSLC1	Transposon vector constructed by ligation of pBSL118 and pHSG396 at *Eco*RI site, Amp^r, Km^r, Cm^r	This study

Amp^r, ampicillin resistance; Cm^r, chloramphenicol resistance, Km^r, kanamycin resistance, Nal^r, nalidixic acid resistance

Table 2 Primer sequences used in this study.

Primer name	Sequence (5'-3')	Purpose
Km-F	TTTACGGTATCGCCGCTCCC	Analysis of transcript
psyI-R1	AGCAACGTAACGGGCATCGT	
lux-1	TGGTGTCTTGTAGCGGCCAG	Amplification of *lux* box
lux-2	GAAAAAGCCGCCGATATCCA	and surrounding region
d*lux*-3	CCGggatccGATTTACCGTTTGAAATACGCG	Deletion of *lux* box
d*lux*-4	CCGggatccCAACACCTTGAAATATAACATTCTG	
mexF-F	GGCTAAGGGACTCGTCCG<u>ATG</u>	Amplification of *mexF*
mexF-R	<u>TCA</u>ATGCATCTCCGCAGGCA	and surrounding region
mexT-F1	TCGACCTCAATCTGCTCATC	RT-PCR for 143 bp of
mexT-R1	GAACAACGGGTCATCGAACA	*mexT* fragment
mexE-F1	CACCTGGGCCAGATGAACTT	RT-PCR for 203 bp of
mexE-R1	AGCACAAACTTCTTGCCCAG	*mexE* fragment
psyI-F	AGGCTGATCAACACCTGTGA	RT-PCR for 234 bp of
psyI-R	CTTGCTGACCACCGTGATG	*psyI* fragment
*Bam*HI-*mexT*	CCCggatccCATGAATCGTAACGACCTGCG	Amplification of *mexT*
mexT-*Eco*RI	CCCgaattcCTATAAACTATCCGGGTCCCC	for overexpression

Underlined letters indicate translation start or stop codons in *mexF*-F and *mexF*-R, respectively. Small letters indicate artificial nucleotide sequence for *Bam*HI in d*lux*-3, d*lux*-4 and *Bam*HI-*mexT* and for *Eco*RI in *mexT*-*Eco*RI, respectively.

Table 3. Gene expression profiles of Δ*fliC*, Δ*fliD*, Δ*motABCD*, Δ*gacA*, Δ*aefR*, and Δ*psyI* strains compared with those of wild-type (WT) strain by microarray analysis

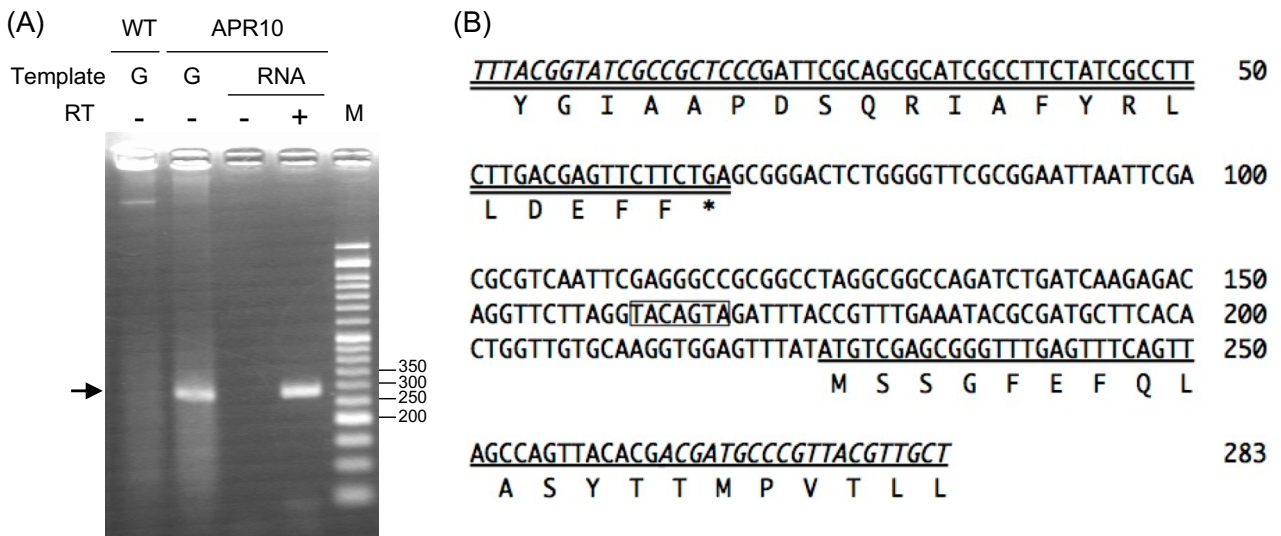| Gene	Δ*fliC*	Δ*motABCD*	Δ*psyI*	Δ*gacA*	Δ*aefR*
psyI	0.02	0.11	0.03	0.16	0.06
psyR	0.06	0.26	0.32	0.26	0.38
mexE	9.91	7.07	7.70	0.78	228.33
mexF	9.64	15.97	12.68	0.83	165.74
oprN	2.77	5.35	3.23	1.01	26.63

Gene expression profiles of AHL production-related mutant strains compared with those of the wild-type (WT) strain. Expression of genes encoding AHL synthase (*psyI*), AHL-binding transcription factor (*psyR*), and components of one of multidrug efflux transporter pump proteins (*mexE*, *mexF* and *oprN*) are indicated as relative values.
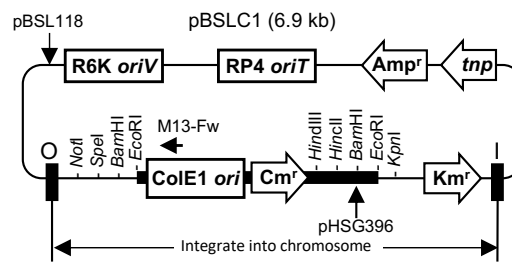
Fig. 1

Fig. 1 Structure of plasmid pBSLC1 used for transposon mutagenesis. Plasmid is not drawn to scale. One of the general-purpose plasmid vectors, pHSG396, and transposon vector pBSL118 were ligated at *Eco*RI. The region between "I" and "O" is randomly inserted into the bacterial genome. The *oriV* and ColE1 *ori* are replication origins of R6K and colicin E1 plasmids, respectively, and *oriT* is an RP4 plasmid-derived conjugative transfer origin. The *tnp* encodes transposase. Amp, ampicillin; Cm, chloramphenicol; Km, kanamycin. The position and direction of the M13-Fw primer are indicated by arrow.
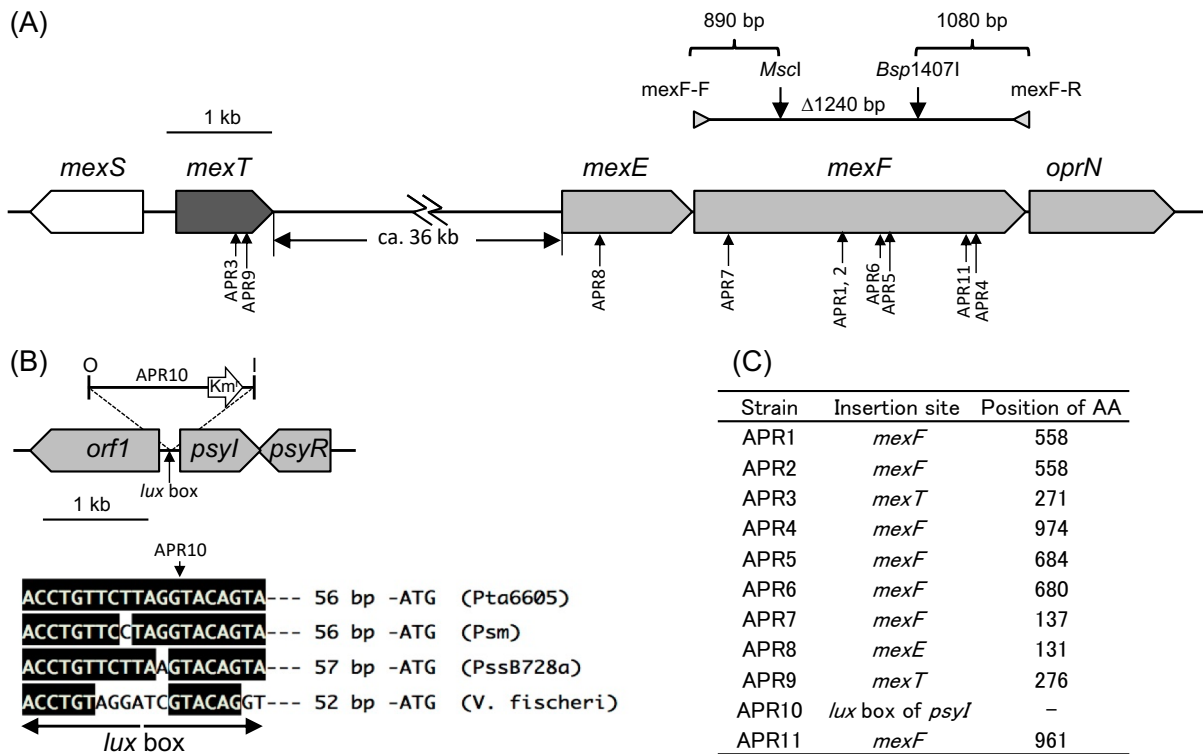
Fig. 2

Fig. 2 Schematic organization of genes into which transposons were inserted. (A) Insertion sites of a transposon in *mexEFoprN* operon and *mexT* gene. There are 1, 7, and 2 insertions in *mexE*, *mexF*, and *mexT*, respectively. Insertion sites are indicated by arrows. Generation of *mexF* mutant is also indicated. (B) Insertion site of a transposon in the *psyI* promoter. The *lux* box, translation start codon ATG, is indicated together with the transposon insertion site. The *lux* boxes from *P. syringae* pv. *maculicola* strain CFBP 10912–9 (*Psm,* Elasri *et al.*, 2001), *P. syringae* pv. *syringae* B728a (PssB728a, Quiñones *et al.*, 2004), and *Vibrio fischeri* ATCC7744 (Devine *et al.*, 1988) are also shown. Arrows below the sequences indicate imperfect inverted repeats. The nucleotides identical to the *lux* box in *Pta*6605 are white on a black background. (C) Insertion sites of all APR strains.
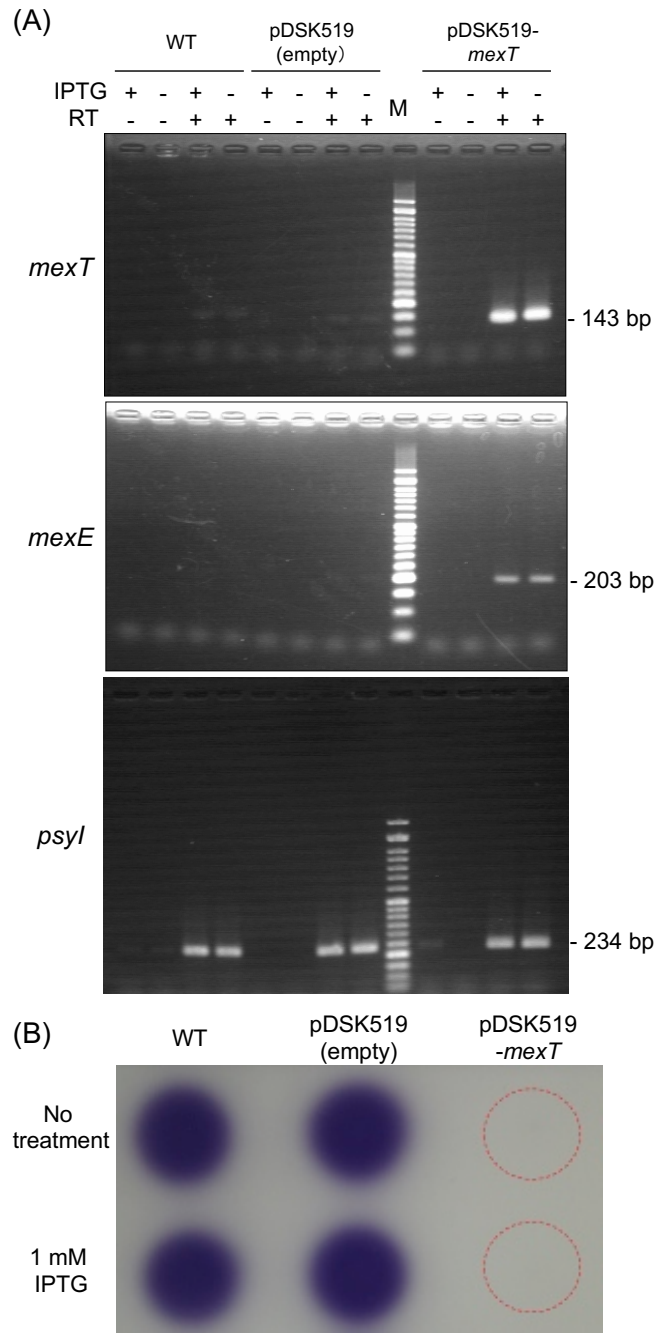
Fig. 3

(A)

	WT	APR10		
Template	G	G	RNA	
RT	−	−	−	+	M

```
—350
—300
—250
—200
```

(B)

```
TTTACGGTATCGCCGCTCCCGATTCGCAGCGCATCGCCTTCTATCGCCTT   50
 Y  G  I  A  A  P  D  S  Q  R  I  A  F  Y  R  L

CTTGACGAGTTCTTCTGAGCGGGACTCTGGGGTTCGCGGAATTAATTCGA  100
 L  D  E  F  F  *

CGCGTCAATTCGAGGGCCGCGGCCTAGGCGGCCAGATCTGATCAAGAGAC  150
AGGTTCTTAGGTACAGTAGATTTACCGTTTGAAATACGCGATGCTTCACA  200
CTGGTTGTGCAAGGTGGAGTTTATATGTCGAGCGGGTTTGAGTTTCAGTT  250
                         M  S  S  G  F  E  F  Q  L

AGCCAGTTACACGACGATGCCCGTTACGTTGCT                    283
 A  S  Y  T  T  M  P  V  T  L  L
```

Fig. 3 RT-PCR analysis of transcript between kanamycin resistance gene and *psyI* in APR10. (A) Genomic DNA (G) of *Pta*6605 wild-type and APR10 was used for PCR as a template. The RT-PCR was carried out using APR10 RNA with/without reverse transcription. Fastgene 50 bp DNA Ladder (Nippon Genetics, Co. LTD, Tokyo Japan) was used as a size marker. (B) Sequence of PCR product. Positions of PCR primers are shown in italic, and part of *lux* box sequence is boxed. The doubly and singly underlined sequences are part of open reading frames for kanamycin resistance gene and *psyI*, respectively. Amino acid sequences are shown below nucleotide sequences. The nucleotide sequence is numbered from side of kanamycin resistance gene.
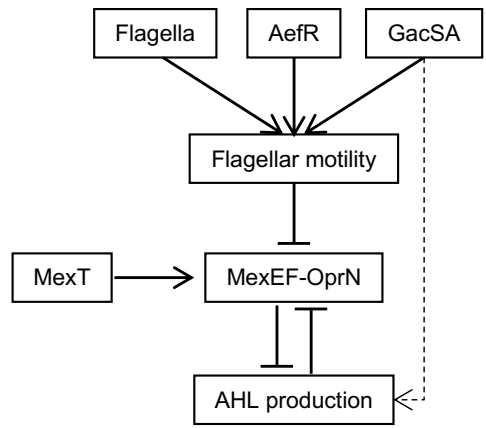
Fig. 4

(A)

(B)
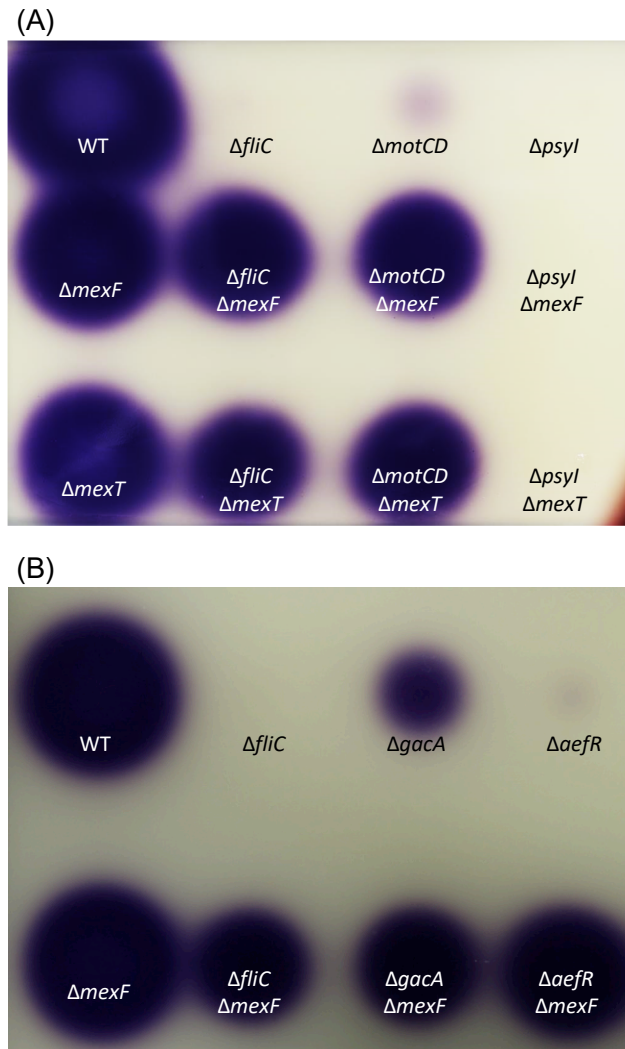
Fig. 4 AHL production in the double mutant strains. AHL was visualized as described in Materials and Methods. (A) Ethyl acetate extract from 1 ml of bacterial culture from Δ*fliC*Δ*mexF*, Δ*motCD*Δ*mexF,* Δ*psyI*Δ*mexF*. Δ*fliC*Δ*mexT*, Δ*motCD*Δ*mexT*, and Δ*psyI*Δ*mexT*, and corresponding single mutant strains and wild-type strain was spotted on the TLC plate. (B) Ethyl acetate extract from 1.5 ml of bacterial culture from Δ*fliC*Δ*mexF*, Δ*gacA*Δ*mexF*, Δ*aefR*Δ*mexF* and corresponding single mutant strains and wild-type strain was spotted on the TLC plate.

Fig. 5

(A)

	WT				pDSK519 (empty)					pDSK519-mexT			
IPTG	+	-	+	-	+	-	+	-	M	+	-	+	-
RT	-	-	+	+	-	-	+	+		-	-	+	+

mexT

- 143 bp

mexE

- 203 bp

psyI

- 234 bp

(B)

	WT	pDSK519 (empty)	pDSK519 -mexT
No treatment			
1 mM IPTG			

Fig. 5 Effect of *mexT*-overexpression on AHL production. (A) Semi-quantitative RT-PCR of *mexT*, *mexE* and *psyI*. PCR for *mexT* and *mexE* was cycled for 25 times, and that for *psyI* was cycled for 30 times. Fastgene 50 bp DNA Ladder (Nippon Genetics) was used as a size marker. (B) AHL production. Ethyl acetate extract from 2 ml of each bacterial culture was spotted on the TLC plate. AHL was visualized as described in Materials and Methods.

Fig. 6

Fig. 6 Schematic depiction of regulatory network for AHL production in *Pta6605*.